Research Article

Numerical and Analytical Study of Optimal Low-Thrust Limited-Power Transfers between Close Circular Coplanar Orbits

Sandro da Silva Fernandes and Wander Almodovar Golfetto

A numerical and analytical study of optimal low-thrust limited-power trajectories for simple transfer (no rendezvous) between close circular coplanar orbits in an inverse-square force field is presented. The numerical study is carried out by means of an indirect approach of the optimization problem in which the two-point boundary value problem, obtained from the set of necessary conditions describing the optimal solutions, is solved through a neighboring extremal algorithm based on the solution of the linearized two-point boundary value problem through Riccati transformation. The analytical study is provided by a linear theory which is expressed in terms of nonsingular elements and is determined through the canonical transformation theory. The fuel consumption is taken as the performance criterion and the analysis is carried out considering various radius ratios and transfer durations. The results are compared to the ones provided by a numerical method based on gradient techniques.

1. Introduction

The main purpose of this paper is to present a numerical and analytical study of optimal low-thrust limited-power trajectories for simple transfers (no rendezvous) between close circular coplanar orbits in an inverse-square force field. The study of these transfers is particularly interesting because the orbits found in practice often have a small eccentricity and the problem of slight modifications (corrections) of these orbits is frequently met [1]. Besides, the analysis has been motivated by the renewed interest in the use of low-thrust propulsion systems in space missions verified in the last two decades. Several researchers have obtained numerical, and sometimes analytical, solutions for a number of specific

initial orbits and specific thrust profiles [2–10]. Averaging methods are also used in such researches [11–15].

Low-thrust electric propulsion systems are characterized by high specific impulse and low-thrust capability and have a great interest for high-energy planetary missions and certain Earth orbit missions. For trajectory calculations, two idealized propulsion models are of most frequent use [1]: LP and CEV systems. In the power-limited variable ejection velocity systems or, simply, LP systems, the only constraint concerns the power, that is, there exists an upper constant limit for the power. In the constant ejection velocity limited-thrust systems or, simply, CEV systems, the magnitude of the thrust acceleration is bounded. In both cases, it is usually assumed that the thrust direction is unconstrained. The utility of these idealized models is that the results obtained from them provide good insight into more realistic problems. In this paper, only LP systems are considered.

In the study presented in the paper, the fuel consumption is taken as the performance criterion and it is calculated for various radius ratios $\rho = r_f/r_0$, where r_0 is the radius of the initial circular orbit O_0 and r_f is the radius of the final circular orbit O_f, and for various transfer durations $t_f - t_0$. Transfers with small and moderate amplitudes are considered. The optimization problem associated to the space transfer problem is formulated as a Mayer problem of optimal control with Cartesian elements—components of position and velocity vectors—as state variables.

The numerical study is carried out by a neighboring extremal algorithm which is based on the linearization about an extremal solution of the nonlinear two-point boundary value problem defined by the set of necessary conditions for a Bolza problem of optimal control with fixed initial and final times, fixed initial state, and constrained final state [16, 17]. The resulting linear two-point boundary value problem is solved through Riccati transformation. As briefly described in Section 2, a slight modification is introduced in the algorithm to improve the convergence. On the other hand, the analytical study is based on a linear theory expressed in terms of nonsingular orbital elements, similar to the ones presented in [1, 18]. Here, the linear theory is determined through canonical transformation theory using the concept of generalized canonical systems. This approach provides a simple way to compare the numerical solutions and the analytical theory. The numerical and analytical results are compared to the ones obtained through an algorithm based on gradient techniques [19, 20].

2. Neighboring extremal algorithm based on Riccati transformation

For completeness, a brief description of the neighboring extremal algorithm used in the paper is presented in this section. This algorithm has a slight modification when compared to the well-known algorithms in the literature [16, 17, 21]: a constraint on the control variations is introduced. Numerical experiments have shown that this simple device improves the convergence.

Let the system of differential equations be defined by

$$\frac{dx_i}{dt} = f_i(x, u), \quad i = 1, \ldots, n, \tag{2.1}$$

where x is an n-vector of state variables and u is an m-vector of control variables. It is assumed that there exist no constraints on the state or control variables. The problem consists in determining the control $u^*(t)$ that transfers the system (2.1) from the initial conditions

$$x(t_0) = x_0, \tag{2.2}$$

to the final conditions at t_f,

$$\psi(x(t_f)) = 0, \tag{2.3}$$

and minimizes the performance index

$$J[u] = g(x(t_f)) + \int_{t_0}^{t_f} F(x,u)dt. \tag{2.4}$$

The functions $f(\cdot) : \mathbb{R}^n \times \mathbb{R}^m \to \mathbb{R}^n$, $F(\cdot) : \mathbb{R}^n \times \mathbb{R}^m \to \mathbb{R}$, $g(\cdot) : \mathbb{R}^n \to \mathbb{R}$, and $\psi(\cdot) : \mathbb{R}^n \to \mathbb{R}^q$, $q < n$, are assumed to be twice continuously differentiable with respect to their arguments. Furthermore, it is assumed that the matrix $[\partial\psi/\partial x]$ has a maximum rank.

By applying the Pontryagin maximum principle [21, 22] to the Bolza problem with constrained final state and fixed terminal times defined by (2.1)–(2.4), the following two-point boundary value problem is obtained:

$$\frac{dx}{dt} = H_\lambda^T, \tag{2.5}$$

$$\frac{d\lambda}{dt} = -H_x^T, \tag{2.6}$$

$$H_u = 0, \tag{2.7}$$

with

$$x(t_0) = x_0, \tag{2.8}$$

$$\lambda(t_f) = -\left(g_x + \mu^T \psi_x\right)^T, \tag{2.9}$$

$$\psi(x(t_f)) = 0, \tag{2.10}$$

where $H(x,\lambda,u) = -F(x,u) + \lambda^T f(x,u)$ is the Hamiltonian function, λ is an n-vector of adjoint variables and μ is a q-vector of Lagrange multipliers. The quantities $H_x, H_u, g_x, \ldots$, and so forth, denote the partial derivatives. If x, λ, and u are taken to be column vectors, then H_x, H_λ, and H_u are row vectors. In this way, ψ_x is a $q \times n$-matrix. The superscript T denotes the transpose of a matrix or a (row or column) vector.

Neighboring extremal methods are iterative procedures used for solving the two-point boundary value problem defined through (2.5)–(2.10). These methods are based on the second variation theory and consist in determining iteratively the unknown adjoint variables $\lambda(t_0)$ and Lagrange multipliers μ. Let $\lambda^0(t_0)$ be an arbitrary starting approximation

of the unknown adjoint variables at t_0. The trajectory $x^0(t)$ corresponding to these starting values is obtained by integrating (2.5) from t_0 to t_f, with the initial conditions (2.8). The vector of Lagrange multipliers μ is then calculated such that the transversality condition (2.9) is fulfilled. Since ψ_x has a maximum rank, one finds that

$$\mu = -\left(\psi_x \psi_x^T\right)^{-1} \psi_x \left(\lambda(t_f) + g_x^T\right). \tag{2.11}$$

Let $\lambda^1(t_0) = \lambda^0(t_0) + \delta\lambda(t_0)$ and $\mu^1 = \mu^0 + \delta\mu$ be the next approximation. Following [16, 21], the corrections (perturbations) $\delta\lambda(t_0)$ and $\delta\mu$ are obtained in order to satisfy the linear two-point boundary value problem obtained from the linearization of (2.5)–(2.10) about a nominal extremal solution defined by $\lambda^0(t_0)$:

$$\delta\dot{x} = H_{\lambda x}\delta x + H_{\lambda u}\delta u, \tag{2.12}$$

$$\delta\dot{\lambda} = -H_{x\lambda}\delta\lambda - H_{xx}\delta x - H_{xu}\delta u, \tag{2.13}$$

$$H_{ux}\delta x + H_{u\lambda}\delta\lambda + H_{uu}\delta u = 0, \tag{2.14}$$

$$\delta x(t_0) = 0, \tag{2.15}$$

$$\psi_x \delta x(t_f) = -k\psi(x(t_f)), \tag{2.16}$$

$$\delta\lambda(t_f) = -\left(g_{xx} + \mu^T \psi_{xx}\right)\delta x(t_f) - \psi_x^T \delta\mu, \tag{2.17}$$

where the constant k, $0 < k \leq 1$, has been introduced to indicate that the correction is partial. Quantities such as $g_{xx}, H_{xx}, H_{x\lambda}, H_{xu}, \ldots$, and so forth, are matrices of second partial derivatives; for instance, $H_{xu} = [\partial^2 H/\partial x_i \partial u_j]$ is an $n \times m$ matrix. According to our notation $H_{\lambda x} = H_{x\lambda}^T$.

Equations (2.12)–(2.17) form the two-point boundary value problem to the accessory minimum problem associated to the original optimization problem defined by (2.1)–(2.4) [16, 17, 21]. This accessory minimum problem is obtained expanding the augmented performance index, which includes through adjoint variables the constraints represented by the state equations, to second order and all constraints to first order, as described in the appendix.

According to the appendix, (2.14) must be replaced by (A.8) since a constraint on the control variations is imposed [23]. Assuming that W_2 is chosen such that $H_{uu} + W_2$ is nonsingular for $t \in \lfloor t_0, t_f \rfloor$, we may solve (A.8) for $\delta u(t)$, in terms of $\delta x(t)$ and $\delta\lambda(t)$:

$$\delta u(t) = -\left(H_{uu} + W_2\right)^{-1}\left(H_{ux}\delta x(t) + H_{u\lambda}\delta\lambda(t)\right). \tag{2.18}$$

Substituting this equation into (2.12) and (2.13), it follows that

$$\delta\dot{x} = A\delta x + B\delta\lambda, \tag{2.19}$$

$$\delta\dot{\lambda} = C\delta x - A^T\delta\lambda, \tag{2.20}$$

where matrices A, B, and C are given by

$$A(t) = H_{\lambda x} - H_{\lambda u}(H_{uu} + W_2)^{-1}H_{ux},$$

$$B(t) = -H_{\lambda u}(H_{uu} + W_2)^{-1}H_{u\lambda}, \tag{2.21}$$

$$C(t) = H_{xu}(H_{uu} + W_2)^{-1}H_{ux} - H_{xx}.$$

We recall that the matrices A, B and C are evaluated on a nominal extremal solution.

Equations (2.15) through (2.20) represent a linear two-point boundary value problem, whose solution can be obtained through a backward sweep method which uses the Riccati transformation [21]:

$$\delta\lambda(t) = R(t)\delta x(t) + L(t)\delta\mu,$$

$$k\psi = L^T(t)\delta x(t) + Q(t)\delta\mu, \tag{2.22}$$

where R is an $n \times n$ symmetric matrix, L is an $n \times q$ matrix, and Q is a $q \times q$ symmetric matrix. For (2.22) to be consistent with (2.15)–(2.20), the Riccati coefficients must satisfy the differential equations (2.23) with the boundary conditions (2.24) defined below.

The step-by-step computing procedure to be used in the neighboring extremal algorithm is summarized as follows.

(1) Guess the starting approximation for $\lambda(t_0)$, that is, $\lambda^0(t_0)$.
(2) The control $u = u(x,\lambda)$ is obtained from (2.7): $H_u = 0$.
(3) Integrate forward, from t_0 to t_f, the system of differential equations (2.5) and (2.6) with the initial conditions $x(t_0) = x_0$ and $\lambda(t_0) = \lambda^0(t_0)$ in order to obtain $x(t_f)$ and $\lambda(t_f)$.
(4) Compute μ through (2.11).
(5) Integrate backward, from t_f to t_0, the differential equations for the Riccati coefficients

$$-\dot{R} = RA + A^T R + RBR - C,$$

$$-\dot{L} = (A^T + RB)L, \tag{2.23}$$

$$-\dot{Q} = L^T BL,$$

with the boundary conditions

$$R(t_f) = -(g_{xx} + \mu^T \psi_{xx}),$$

$$L(t_f) = -\psi_x^T, \tag{2.24}$$

$$Q(t_f) = 0,$$

and the system of differential equations (2.5) and (2.6) with boundary conditions $x(t_f)$ and $\lambda(t_f)$.
(6) Compute the variation $\delta\mu$ from $\delta\mu = Q(t_0)^{-1}k\psi$.

(7) Compute $\delta\lambda(t_0)$ from $\delta\lambda(t_0) = L(t_0)\delta\mu$.

(8) Test the convergence. If it is not obtained, update the unknown $\lambda(t_0)$, that is, compute the new value $\lambda^1(t_0) = \lambda^0(t_0) + \delta\lambda(t_0)$.

(9) Go back to step 2 and repeat the procedure until convergence is achieved.

3. Optimal low-thrust trajectories

In what follows, the neighboring extremal algorithm presented in previous section is applied to determine optimal low-thrust limited-power transfers between close coplanar circular orbits in an inverse-square force field.

3.1. Problem formulation. A low-thrust limited-power propulsion system, or LP system, is characterized by low-thrust acceleration level and high specific impulse [1]. The ratio between the maximum thrust acceleration and the gravity acceleration on the ground, γ_{max}/g_0, is between 10^{-4} and 10^{-2}. For such system, the fuel consumption is described by the variable J defined as

$$J = \frac{1}{2} \int_{t_0}^{t_f} \gamma^2 dt, \tag{3.1}$$

where γ is the magnitude of the thrust acceleration vector $\boldsymbol{\Gamma}$, used as control variable. The consumption variable J is a monotonic decreasing function of the mass m of the space vehicle:

$$J = P_{max} \left(\frac{1}{m} - \frac{1}{m_0} \right), \tag{3.2}$$

where P_{max} is the maximum power and m_0 is the initial mass. The minimization of the final value of the fuel consumption J_f is equivalent to the maximization of m_f.

The optimization problem concerned with simple transfers (no rendezvous) between coplanar orbits will be formulated as a Mayer problem of optimal control by using Cartesian elements as state variables. At time t, the state of a space vehicle M is defined by the radial distance r from the center of attraction, the radial and transverse components of the velocity, u and v, and the fuel consumption J. (Note that the radial component u should not be confused with the control variables defined in Section 2.) The geometry of the transfer problem is illustrated in Figure 3.1.

In the two-dimension optimization problem, the state equations are given by

$$\frac{du}{dt} = \frac{v^2}{r} - \frac{\mu}{r^2} + R,$$

$$\frac{dv}{dt} = -\frac{uv}{r} + S,$$

$$\frac{dr}{dt} = u, \tag{3.3}$$

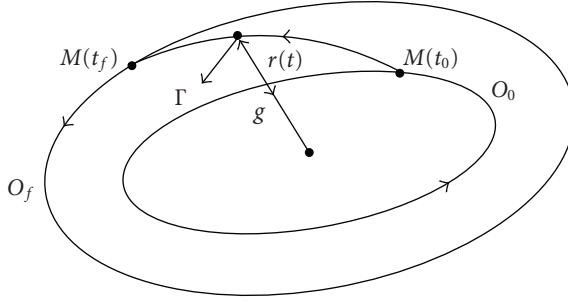$$\frac{dJ}{dt} = \frac{1}{2}(R^2 + S^2),$$

Figure 3.1. Geometry of transfer problem.

where μ is the gravitational parameter (it should not be confused with Lagrange multiplier defined in Section 2), R and S are the components of the thrust acceleration vector in a moving frame of reference, that is, $\mathbf{\Gamma} = R\mathbf{e}_r + S\mathbf{e}_s$, with the unit vector $\mathbf{e}_r$ pointing radially outward and the unit vector $\mathbf{e}_s$ perpendicular to $\mathbf{e}_r$ in the direction of the motion and in the plane of orbit. The optimization problem is stated as follows: it is proposed to transfer a space vehicle M from the initial conditions at t_0,

$$u(0) = 0, \qquad v(0) = 1, \qquad r(0) = 1, \qquad J(0) = 0, \tag{3.4}$$

to the final state at the prescribed final time t_f,

$$u(t_f) = 0, \qquad v(t_f) = \sqrt{\frac{\mu}{r_f}}, \qquad r(t_f) = r_f, \tag{3.5}$$

such that J_f is a minimum.

We note that in the formulation of the boundary conditions above all variables are dimensionless. In this case, $\mu = 1$.

3.2. Two-point boundary value problem. Following the Pontryagin maximum principle [21, 22], the adjoint variables λ_u, λ_v, λ_r, and λ_J are introduced and the Hamiltonian function $H(u,v,r,J,\lambda_u,\lambda_v,\lambda_r,\lambda_J,R,S)$ is formed using the right-hand side of (3.3):

$$H = \lambda_u\left(\frac{v^2}{r} - \frac{\mu}{r^2} + R\right) + \lambda_v\left(-\frac{uv}{r} + S\right) + \lambda_r u + \frac{\lambda_J}{2}\left(R^2 + S^2\right). \tag{3.6}$$

The control variables R and S must be selected from the admissible controls such that the Hamiltonian function reaches its maximum along the optimal trajectory. Thus, we find that

$$R^* = -\frac{\lambda_u}{\lambda_J}$$

$$\tag{3.7}$$

$$S^* = -\frac{\lambda_v}{\lambda_J}.$$

The variables λ_u, λ_v, λ_r, and λ_J must satisfy the adjoint differential equations and the transversality conditions (2.6) and (2.9).

Therefore, from (3.3)–(3.7), we get the following two-point boundary value problem for the transfer problem defined by (3.3)–(3.5):

$$\frac{du}{dt} = \frac{v^2}{r} - \frac{\mu}{r^2} - \frac{\lambda_u}{\lambda_J}, \qquad \frac{dv}{dt} = -\frac{uv}{r} - \frac{\lambda_v}{\lambda_J},$$

$$\frac{dr}{dt} = u, \qquad \frac{dJ}{dt} = \frac{1}{2\lambda_J^2}\left(\lambda_u^2 + \lambda_v^2\right),$$

$$\frac{d\lambda_u}{dt} = \frac{v}{r}\lambda_v - \lambda_r, \qquad \frac{d\lambda_v}{dt} = -2\frac{v}{r}\lambda_u + \frac{u}{r}\lambda_v,$$

$$\frac{d\lambda_r}{dt} = \left(\frac{v^2}{r^2} - 2\frac{\mu}{r^3}\right)\lambda_u - \frac{uv}{r^2}\lambda_v, \qquad \frac{d\lambda_J}{dt} = 0,$$

(3.8)

with the boundary conditions given by (3.4) and (3.5), and the transversality condition

$$\lambda_J(t_f) = -1.$$

(3.9)

3.3. Applying the neighboring extremal algorithm. The matrices A, B, and C describing the linearized two-point boundary value problem in the neighboring extremal algorithm can be obtained straightforwardly from (3.8) by calculating the partial derivatives of the right-hand side of the equation with respect to the state and adjoint variables taking into account a diagonal weighting matrix W_2 as described in the next paragraph. These matrices are then given by

$$A = \begin{bmatrix} 0 & \dfrac{2v}{r} & -a & 0 \\ -\dfrac{v}{r} & -\dfrac{u}{r} & \dfrac{uv}{r^2} & 0 \\ 1 & 0 & 0 & 0 \\ 0 & 0 & 0 & 0 \end{bmatrix}, \qquad B = \begin{bmatrix} -\dfrac{1}{\lambda_J - \sigma} & 0 & 0 & \dfrac{\lambda_u}{\lambda_J(\lambda_J - \sigma)} \\ 0 & -\dfrac{1}{(\lambda_J - \sigma)} & 0 & \dfrac{\lambda_v}{\lambda_J(\lambda_J - \sigma)} \\ 0 & 0 & 0 & 0 \\ \dfrac{\lambda_u}{\lambda_J(\lambda_J - \sigma)} & \dfrac{\lambda_v}{\lambda_J(\lambda_J - \sigma)} & 0 & -\dfrac{c}{\lambda_J^2(\lambda_J - \sigma)} \end{bmatrix},$$

$$C = \begin{bmatrix} 0 & \dfrac{\lambda_v}{r} & -\dfrac{v\lambda_v}{r^2} & 0 \\ \dfrac{\lambda_v}{r} & -\dfrac{2\lambda_u}{r} & b & 0 \\ -\dfrac{v\lambda_v}{r^2} & b & d & 0 \\ 0 & 0 & 0 & 0 \end{bmatrix},$$

(3.10)

where

$$a = \frac{v^2}{r^2} - 2\frac{\mu}{r^3}, \qquad b = \frac{2v}{r^2}\lambda_u - \frac{u}{r^2}\lambda_v,$$

$$c = \lambda_u^2 + \lambda_v^2, \qquad d = \left(-\frac{2v^2}{r^3} + \frac{6\mu}{r^4}\right)\lambda_u + \frac{2uv}{r^3}\lambda_v. \tag{3.11}$$

In Section 5, we present the results obtained through the neighboring extremal algorithm for several ratios $\rho = r_f/r_0$, $\rho = 0.727; 0.800; 0.900; 0.950; 0.975; 1.025; 1.050; 1.100;$ $1.200; 1.523$, and nondimensional transfer durations of 2, 3, 4, 5. We note that the Earth-Mars transfer corresponds to $\rho = 1.523$ and Earth-Venus to $\rho = 0.727$. The criterion adopted for convergence is a tolerance of 1.0×10^{-8} in the computation of corrections (variations) of the initial value of the adjoint variables. In view of this convergence criterion, the terminal constraints are obtained with an error less than 1.0×10^{-6}, which means that $\|\psi(x(t_f))\| \le 1.0 \times 10^{-6}$. All simulations consider the transfer from low orbit to high orbit, with starting approximation $\lambda^0(t_0) = (0.001 \quad 0.001 \quad 0.001 \quad -1)$, attenuation factor $k = 0.10$ for $\rho = 0.727$ and 1.5236, and $k = 0.15$ for the other values of ρ, and a diagonal matrix W_2 such that $W_{2_{11}} = W_{2_{22}} = -\sigma$, with $\sigma = 5.5$ for all maneuvers, except $\rho = 0.727$ and 0.800, with $t_f - t_0 = 4$ and 5. In these cases, $\sigma = 2.5$.

4. Linear theory

In this section, a first-order analytical solution for the problem of optimal simple transfer defined in Section 3.1 is presented.

The Hamiltonian function H^* governing the extremal (optimal) trajectories can be obtained as follows. Since λ_J is a first integral (3.8) and $\lambda_J(t_f) = -1$, from the transversality condition (3.9), it follows that $\lambda_J(t) = -1$. Thus, from (3.7), we find the optimal thrust acceleration

$$R^* = \lambda_u, \qquad S^* = \lambda_v. \tag{4.1}$$

Introducing these equations into (3.6), it results that

$$H^* = u\lambda_r + \left(\frac{v^2}{r} - \frac{\mu}{r^2}\right)\lambda_u - \frac{uv}{r}\lambda_v + \frac{1}{2}(\lambda_u^2 + \lambda_v^2). \tag{4.2}$$

In what follows, we consider the problem of determining an approximate solution of the system of differential equations governed by the Hamiltonian H^* by means of the theory of canonical transformations. This analytical solution is obtained through the canonical transformation theory using the concept of generalized canonical systems [24, 25].

Now, consider the Hamiltonian function describing a null thrust arc in the two-dimensional formulation of the optimization problem defined in Section 3.1:

$$H = u\lambda_r + \left(\frac{v^2}{r} - \frac{\mu}{r^2}\right)\lambda_u - \frac{uv}{r}\lambda_v + \frac{v}{r}\lambda_\theta. \tag{4.3}$$

Note that H is obtained from (3.6) taking $R = S = 0$ and adding the last term concerning the differential equation of the angular variable θ, which defines the position of the space vehicle with respect to a reference axis in the plane of motion. This variable is important for rendezvous problems and plays no special role for simple transfer problems like the one considered here, but it is necessary to define the canonical transformations described below. In the transformation theory described in the next paragraphs, it is assumed that the Hamiltonian H^* is augmented in order to include this last term, that is,

$$H^* = u\lambda_r + \left(\frac{v^2}{r} - \frac{\mu}{r^2}\right)\lambda_u - \frac{uv}{r}\lambda_v + \frac{v}{r}\lambda_\theta + \frac{1}{2}(\lambda_u^2 + \lambda_v^2). \tag{4.4}$$

Note that H is the undisturbed part of H^* and plays a fundamental role in our theory.

According to the properties of generalized canonical systems, the general solution of the system of differential equations governed by the Hamiltonian H can be expressed in terms of a fast phase and is given by [24, 25]:

$$
\begin{aligned}
u &= \sqrt{\frac{\mu}{p}} e \sin f, \\[2mm]
v &= \sqrt{\frac{\mu}{p}} (1 + e \cos f), \\[2mm]
r &= \frac{p}{1 + e \cos f}, \\[2mm]
\theta &= \omega + f, \\[2mm]
\lambda_u &= \sqrt{\frac{p}{\mu}} \sin f \, \lambda_e + \sqrt{\frac{p}{\mu}} \frac{\cos f}{e} (\lambda_f - \lambda_\omega) \\[2mm]
\lambda_v &= 2\sqrt{\frac{p}{\mu}} r \lambda_p + \sqrt{\frac{p}{\mu}} (2\cos f + e\cos^2 f + e) \frac{r}{p} \lambda_e - \sqrt{\frac{p}{\mu}} \frac{\sin f}{e} \left[1 + \frac{r}{p}\right] (\lambda_f - \lambda_\omega), \\[2mm]
\lambda_r &= 2\frac{p}{r} \lambda_p + \frac{\cos f + e}{r} \lambda_e - \frac{\sin f}{re} (\lambda_f - \lambda_\omega), \\[2mm]
\lambda_\theta &= \lambda_\omega,
\end{aligned}
\tag{4.5}
$$

where p is the semi latus rectum, e is the eccentricity, ω is the pericenter argument, f is the true anomaly (fast phase), and $(\lambda_p, \lambda_e, \lambda_f, \lambda_\omega)$ are adjoint variables to (p, e, f, ω).

Equations (4.5) define a Mathieu transformation between the Cartesian elements and the orbital ones,

$$(u, v, r, \theta, \lambda_u, \lambda_v, \lambda_r, \lambda_\theta) \xrightarrow{\text{Mathieu}} (p, e, f, \omega, \lambda_p, \lambda_e, \lambda_f, \lambda_\omega). \tag{4.6}$$

The undisturbed Hamiltonian function H is invariant with respect to this canonical transformation. Thus, the undisturbed Hamiltonian is written in terms of the new variables as

$$H = \frac{\sqrt{\mu p}}{r^2}\lambda_f. \tag{4.7}$$

The general solution of the new differential equations governed by the new undisturbed Hamiltonian function H is closely related to the solution of time flight equation in the two-body problem for elliptic, parabolic, and hyperbolic motions [25]. For quasicircular motions, this solution is very simple, as described in the next paragraphs.

Equations (4.5) have singularities for circular orbits ($e = 0$). In order to avoid this drawback, a set of nonsingular elements is introduced. The relationships between the singular orbital elements and the nonsingular ones are given by

$$a = \frac{p}{(1-e^2)}, \qquad h = e\cos\omega, \qquad k = e\sin\omega, \qquad L = f + \omega. \tag{4.8}$$

These equations define a Lagrange point transformation and the Jacobian of the inverse of this transformation must be computed in order to get the relationships between the corresponding adjoint variables. Thus, we get

$$\begin{aligned}
\lambda_a &= (1-e^2)\lambda_p, \\
\lambda_h &= \left(\lambda_e - \frac{2ep}{(1-e^2)}\lambda_p\right)\cos\omega + \left(\frac{\lambda_L - \lambda_\omega}{e}\right)\sin\omega, \\
\lambda_k &= \left(\lambda_e - \frac{2ep}{(1-e^2)}\lambda_p\right)\sin\omega - \left(\frac{\lambda_L - \lambda_\omega}{e}\right)\cos\omega, \\
\lambda_L &= \lambda_f.
\end{aligned} \tag{4.9}$$

Equations (4.8) and (4.9) define a new Mathieu transformation between singular and nonsingular elements,

$$(p, e, f, \omega, \lambda_p, \lambda_e, \lambda_f, \lambda_\omega) \xrightarrow{\text{Mathieu}} (a, h, k, L, \lambda_a, \lambda_h, \lambda_k, \lambda_L). \tag{4.10}$$

Substituting (4.8) and (4.9) into (4.5), we get

$$u = \sqrt{\frac{\mu}{a(1-h^2-k^2)}}(h\sin L - k\cos L),$$

$$v = \sqrt{\frac{\mu}{a(1-h^2-k^2)}}(1 + h\cos L + k\sin L),$$

$$r = \frac{a(1-h^2-k^2)}{1 + h\cos L + k\sin L},$$
$$\theta = L,$$

$$\lambda_u = \sqrt{\frac{a}{\mu}} \left\{ 2a\lambda_a \frac{(h\sin L - k\cos L)}{\sqrt{1 - h^2 - k^2}} + \sqrt{1 - h^2 - k^2}\,(\lambda_h \sin L - \lambda_k \cos L) \right\},$$

$$\lambda_v = \sqrt{\frac{a}{\mu}} \left\{ 2a\lambda_a \sqrt{1 - h^2 - k^2}\left(\frac{a}{r}\right) \right.$$

$$+ \frac{1}{\sqrt{1 - h^2 - k^2}}\left(\frac{r}{a}\right)\left\{ \left[\frac{3}{2}h + 2\cos L + \frac{h}{2}\cos 2L + \frac{k}{2}\sin 2L\right]\lambda_h \right.$$

$$\left.\left. + \left[\frac{3}{2}k + 2\sin L - \frac{k}{2}\cos 2L + \frac{h}{2}\sin 2L\right]\lambda_k\right\} \right\},$$

$$\lambda_r = 2\left(\frac{a}{r}\right)^2 \lambda_a + \frac{1}{r}\left[(h + \cos L)\lambda_h + (k + \sin L)\lambda_k\right],$$

$$\lambda_\theta = -k\lambda_h + h\lambda_k + \lambda_L.$$

$$(4.11)$$

These equations are valid for all orbits and define a Mathieu transformation between the Cartesian elements and the nonsingular orbital elements.

For quasicircular orbits, with very small eccentricities, (4.11) can be greatly simplified if higher-order terms in eccentricity are neglected. Thus,

$$u = na(h\sin\ell - k\cos\ell),$$

$$v = na(1 + h\cos\ell + k\sin\ell),$$

$$r = \frac{a}{1 + h\cos\ell + k\sin\ell},$$

$$\theta = \ell$$

$$\lambda_u = \frac{1}{na}(\lambda_h \sin\ell - \lambda_k \cos\ell),$$

$$(4.12)$$

$$\lambda_v = \frac{2}{na}\left[a\lambda_a + (\lambda_h \cos\ell + \lambda_k \sin\ell)\right],$$

$$\lambda_r = 2\lambda_a + \frac{1}{a}(\lambda_h \cos\ell + \lambda_k \sin\ell),$$

$$\lambda_\theta = \lambda_\ell,$$

where $n = \sqrt{\mu/a^3}$ is the mean motion and $\ell = \omega + M$ is the mean latitude. We note that first-order terms in eccentricity are retained in the state variables in order to get a trajectory with better accuracy. For adjoint variables, this is unnecessary since λ_a, λ_h, and λ_k are small quantities for transfers between close circular orbits, that is, for small amplitude transfers.

Introducing (4.12) into the expression for H^*, we finally get

$$
\begin{aligned}
H^* = n\lambda_\ell + \frac{1}{2n^2 a^2} \Bigg\{ & 4a^2\lambda_a^2 + \frac{5}{2}(\lambda_h^2 + \lambda_k^2) + 8a\lambda_a\lambda_k \sin\ell + 8a\lambda_a\lambda_h \cos\ell \\
& + 3\lambda_h\lambda_k \sin 2\ell + \frac{3}{2}(\lambda_h^2 - \lambda_k^2)\cos 2\ell \Bigg\}.
\end{aligned}
\tag{4.13}
$$

For transfers between close circular coplanar orbits, an approximate solution of the system of differential equations governed by H^* can be obtained through simple integrations if the system is linearized about a reference circular orbit $\overline{O}$ with semimajor axis $\overline{a}$. This solution can be put in the form

$$
\Delta x = A\lambda_0,
\tag{4.14}
$$

where $\Delta x = [\Delta\alpha \quad \Delta h \quad \Delta k]^T$ denotes the imposed changes on nonsingular orbital elements (state variables), $\alpha = a/\overline{a}$, $\lambda_\alpha = \overline{a}\lambda_a$, λ_0 is the 3×1 vector of initial values of the adjoint variables, and A is a 3×3 symmetric matrix. The adjoint variables are constant and the matrix A is given by

$$
A = \begin{bmatrix} a_{\alpha\alpha} & a_{\alpha h} & a_{\alpha k} \\ a_{h\alpha} & a_{hh} & a_{hk} \\ a_{k\alpha} & a_{kh} & a_{kk} \end{bmatrix},
\tag{4.15}
$$

where

$$
a_{\alpha\alpha} = 4\sqrt{\frac{\overline{a}^5}{\mu^3}}\,\Delta\overline{\ell},
\tag{4.16}
$$

$$
a_{\alpha h} = a_{h\alpha} = 4\sqrt{\frac{\overline{a}^5}{\mu^3}}\,(\sin\overline{\ell}_f - \sin\overline{\ell}_0),
\tag{4.17}
$$

$$
a_{\alpha k} = a_{k\alpha} = -4\sqrt{\frac{\overline{a}^5}{\mu^3}}\,(\cos\overline{\ell}_f - \cos\overline{\ell}_0),
\tag{4.18}
$$

$$
a_{hh} = \sqrt{\frac{\overline{a}^5}{\mu^3}}\left[\frac{5}{2}\Delta\overline{\ell} + \frac{3}{4}(\sin 2\overline{\ell}_f - \sin 2\overline{\ell}_0)\right],
\tag{4.19}
$$

$$
a_{hk} = a_{kh} = -\frac{3}{4}\sqrt{\frac{\overline{a}^5}{\mu^3}}\,(\cos 2\overline{\ell}_f - \cos 2\overline{\ell}_0),
\tag{4.20}
$$

$$
a_{kk} = \sqrt{\frac{\overline{a}^5}{\mu^3}}\left[\frac{5}{2}\Delta\overline{\ell} - \frac{3}{4}(\sin 2\overline{\ell}_f - \sin 2\overline{\ell}_0)\right].
\tag{4.21}
$$

Subscript f stands for the final time, $\overline{\ell} = \overline{\ell}_0 + \overline{n}(t - t_0)$, and t_0 is the initial time. The linear solution, described by (4.14)–(4.21), is in agreement with the one presented in [1, 18], where it is obtained through a different approach.

In view of (4.1) and (4.12), the optimal thrust acceleration $\mathbf{\Gamma}^*$ is expressed by

$$\mathbf{\Gamma}^* = \frac{1}{na}\{(\lambda_h \sin\overline{\ell} - \lambda_k \cos\overline{\ell})\mathbf{e}_r + 2(\lambda_\alpha + \lambda_h \cos\overline{\ell} + \lambda_k \sin\overline{\ell})\mathbf{e}_s\}. \tag{4.22}$$

The variation of the consumption variable ΔJ during the maneuver can be obtained straightforwardly from (4.13) and (4.15) by integrating, from t_0 to t_f, the differential equation (see (3.3), (4.1), and (4.13))

$$\frac{dJ}{dt} = H_\gamma^*, \tag{4.23}$$

where H_γ^* denotes the part of the Hamiltonian H^* concerned with the thrust acceleration. Thus,

$$\Delta J = \frac{1}{2}\{a_{\alpha\alpha}\lambda_\alpha^2 + 2a_{\alpha h}\lambda_\alpha\lambda_h + 2a_{\alpha k}\lambda_\alpha\lambda_k + a_{hh}\lambda_h^2 + 2a_{hk}\lambda_h\lambda_k + a_{kk}\lambda_k^2\}, \tag{4.24}$$

where $a_{\alpha\alpha}, a_{\alpha h}, \ldots, a_{kk}$ are given by (4.16)–(4.21); and λ_α, λ_h, and λ_k are obtained from the solution of the linear algebraic system defined by (4.14).

We recall that the extremal (optimal) trajectory is given by (4.12) with the nonsingular elements a, h, and k calculated from (4.14).

For transfers between circular orbits, only $\Delta\alpha$ is imposed. If it is assumed that the initial and final positions of the vehicle in orbit are symmetric with respect to x-axis of the inertial reference frame, that is, $\overline{\ell}_f = -\overline{\ell}_0 = \Delta\ell/2$, the solution of the system (4.14) is given by

$$\lambda_\alpha = \frac{1}{2}\sqrt{\frac{\mu^3}{\overline{a}^5}}\left\{\frac{\Delta\alpha(5\Delta\overline{\ell} + 3\sin\Delta\overline{\ell})}{10\Delta\overline{\ell}^2 + 6\Delta\overline{\ell}\sin\Delta\overline{\ell} - 64\sin^2(\Delta\overline{\ell}/2)}\right\},$$

$$\lambda_h = -\sqrt{\frac{\mu^3}{\overline{a}^5}}\left\{\frac{8\Delta\alpha\sin(\Delta\overline{\ell}/2)}{10\Delta\overline{\ell}^2 + 6\Delta\overline{\ell}\sin\Delta\overline{\ell} - 64\sin^2(\Delta\overline{\ell}/2)}\right\}, \tag{4.25}$$

$$\lambda_k = 0.$$

We note that the linear theory is applicable only to orbits which are not separated by large radial distance, that is, to transfers between close orbits. If the reference orbit is chosen in the conventional way, that is, with the semimajor axis as the radius of the initial orbit, the radial excursion to the final orbit will be maximized [26]. A better reference orbit is defined with a semimajor axis given by an intermediate value between the values of semimajor axes of the terminal orbits. In our analysis, we have chosen $\overline{a} = (a_0 + a_f)/2$ in order to improve the accuracy in the calculations.

In the next section, the results of the linear theory are compared to the ones provided by the neighboring extremal algorithm described in Sections 2 and 3.

Table 5.1. Consumption variable J ($\rho > 1$).

ρ	$t_f - t_0$	J_{anal}	J_{grad}	J_{neigh}	d_{rel1}	d_{rel2}
	2.0	3.5856×10^{-4}	3.5855×10^{-4}	3.5854×10^{-4}	0.00	0.00
	3.0	8.4459×10^{-5}	8.4462×10^{-5}	8.4456×10^{-5}	0.00	0.01
1.0250	4.0	3.1226×10^{-5}	3.1233×10^{-5}	3.1230×10^{-5}	0.01	0.01
	5.0	1.7138×10^{-5}	1.7147×10^{-5}	1.7143×10^{-5}	0.03	0.02
	2.0	1.4463×10^{-3}	1.4463×10^{-3}	1.4459×10^{-3}	0.03	0.03
	3.0	3.4169×10^{-4}	3.4166×10^{-4}	3.4164×10^{-4}	0.02	0.01
1.0500	4.0	1.2533×10^{-4}	1.2538×10^{-4}	1.2537×10^{-4}	0.03	0.00
	5.0	6.7541×10^{-5}	6.7611×10^{-5}	6.7598×10^{-5}	0.08	0.02
	2.0	5.8778×10^{-3}	5.8741×10^{-3}	5.8716×10^{-3}	0.11	0.04
	3.0	1.3977×10^{-3}	1.3970×10^{-3}	1.3969×10^{-3}	0.06	0.00
1.1000	4.0	5.0619×10^{-4}	5.0666×10^{-4}	5.0664×10^{-4}	0.09	0.00
	5.0	2.6374×10^{-4}	2.6453×10^{-4}	2.6451×10^{-4}	0.29	0.01
	2.0	2.4187×10^{-2}	2.4097×10^{-2}	2.4097×10^{-2}	0.37	0.00
	3.0	5.8370×10^{-3}	5.8200×10^{-3}	5.8199×10^{-3}	0.29	0.00
1.2000	4.0	2.0813×10^{-3}	2.0845×10^{-3}	2.0844×10^{-3}	0.15	0.00
	5.0	1.0260×10^{-3}	1.0346×10^{-3}	1.0345×10^{-3}	0.83	0.00
	2.0	1.7743×10^{-1}	1.7434×10^{-1}	1.7434×10^{-1}	1.77	0.00
	3.0	4.4947×10^{-2}	4.4067×10^{-2}	4.4066×10^{-2}	1.99	0.00
1.5236	4.0	1.6051×10^{-2}	1.5889×10^{-2}	1.5889×10^{-2}	1.02	0.00
	5.0	7.2498×10^{-3}	7.3352×10^{-3}	7.3351×10^{-3}	1.17	0.00

5. Results

The values of the consumption variable J computed through the neighboring extremal algorithm and the ones provided by the linear theory and by a numerical method based on gradient techniques [19] are presented in Tables 5.1 and 5.2, and are plotted in Figures 5.1 and 5.2, as function of the radius ratio ρ of the terminal orbits for various transfer durations $t = t_f - t_0$. The absolute relative difference in percent between the numerical and analytical results is also presented in the tables according to the following definition:

$$d_{rel1} = \left| \frac{J_{neigh} - J_{linear}}{J_{neigh}} \right| \times 100\%,$$

$$d_{rel2} = \left| \frac{J_{neigh} - J_{grad}}{J_{neigh}} \right| \times 100\%. \tag{5.1}$$

Tables 5.1 and 5.2 show that $d_{rel1} < 2\%$ for $\rho > 1$, and $d_{rel1} < 5.5\%$ for $\rho < 1$. The greater values corresponds to transfers with moderate amplitude $\rho = 0.7270$ and $\rho = 1.5236$. On the other hand, $d_{rel2} < 0.04\%$ for all cases.

Tables 5.1 and 5.2, and Figures 5.1 and 5.2 show the good agreement between the results. Note that the linear theory provides a good approximation for the solution of the

Table 5.2. Consumption variable J ($\rho < 1$).

ρ	$t_f - t_0$	J_{linear}	J_{grad}	J_{neigh}	d_{rel1}	d_{rel2}
0.7270	2.0	3.7654×10^{-2}	3.7299×10^{-2}	3.7298×10^{-2}	0.95	0.00
	3.0	8.9269×10^{-3}	9.0261×10^{-3}	9.0259×10^{-3}	1.10	0.00
	4.0	4.0482×10^{-3}	4.2133×10^{-3}	4.2131×10^{-3}	3.91	0.00
	5.0	2.8941×10^{-3}	3.0573×10^{-3}	3.0572×10^{-3}	5.33	0.00
0.8000	2.0	2.0951×10^{-2}	2.0842×10^{-2}	2.0842×10^{-2}	0.52	0.00
	3.0	4.9040×10^{-3}	4.9173×10^{-3}	4.9172×10^{-3}	0.27	0.00
	4.0	2.0703×10^{-3}	2.1047×10^{-3}	2.1046×10^{-3}	1.63	0.00
	5.0	1.3838×10^{-3}	1.4198×10^{-3}	1.4197×10^{-3}	2.53	0.00
0.9000	2.0	5.4740×10^{-3}	5.4672×10^{-3}	5.4671×10^{-3}	0.13	0.00
	3.0	1.2771×10^{-3}	1.2772×10^{-3}	1.2771×10^{-3}	0.00	0.01
	4.0	5.0063×10^{-4}	5.0198×10^{-4}	5.0198×10^{-4}	0.27	0.00
	5.0	3.0496×10^{-4}	3.0653×10^{-4}	3.0652×10^{-4}	0.51	0.00
0.9500	2.0	1.3958×10^{-3}	1.3955×10^{-3}	1.3955×10^{-3}	0.02	0.00
	3.0	3.2649×10^{-4}	3.2649×10^{-4}	3.2647×10^{-4}	0.01	0.01
	4.0	1.2451×10^{-4}	1.2459×10^{-4}	1.2458×10^{-4}	0.06	0.00
	5.0	7.2585×10^{-5}	7.2671×10^{-5}	7.2667×10^{-5}	0.11	0.01
0.9750	2.0	3.5225×10^{-4}	3.5231×10^{-4}	3.5223×10^{-4}	0.01	0.02
	3.0	8.2555×10^{-5}	8.2560×10^{-5}	8.2553×10^{-5}	0.00	0.01
	4.0	3.1120×10^{-5}	3.1126×10^{-5}	3.1124×10^{-5}	0.01	0.01
	5.0	1.7765×10^{-5}	1.7772×10^{-5}	1.7771×10^{-5}	0.03	0.00

low-thrust limited-power transfer between close circular coplanar orbits in an inverse-square force field.

Figures 5.1 and 5.2 also show that the fuel consumption can be greatly reduced if the duration of the transfer is increased. The fuel consumption for transfers with duration $t_f - t_0 = 2$ is approximately ten times the fuel consumption for a transfer with duration $t_f - t_0 = 4$.

In order to follow the evolution of the optimal thrust acceleration vector during the transfer, it is convenient to plot the locus of its tip in the moving frame of reference. Figures 5.3 and 5.4 illustrate these plots for small amplitude transfers with $\rho = 0.950$ and 1.050, and for moderate amplitude transfers, Earth-Mars ($\rho = 1.523$), and Earth-Venus ($\rho = 0.727$) transfers, with $t_f - t_0 = 2$. It should be noted that the agreement between the numerical and analytical results is better for small amplitude transfers. For moderate amplitude transfers, this difference increases with the duration of the maneuvers.

Figures 5.5 and 5.6 show the time history of the state variables—u, v, and r—for a small amplitude transfer, $\rho = 1.050$, and a moderate amplitude transfer, $\rho = 1.523$, with $t_f - t_0 = 2$. Again, the agreement between the numerical and analytical results is better for small amplitude transfers.
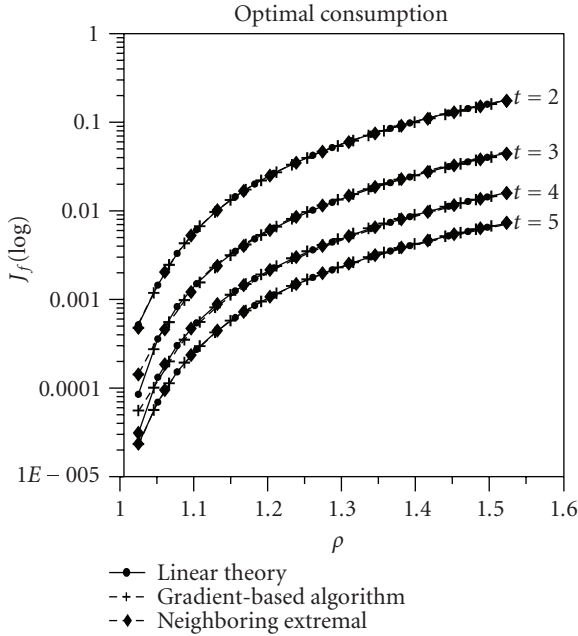
Figure 5.1. Consumption variable J for $\rho > 1$.

The results—consumption variable, thrust acceleration, and trajectory—provided by the gradient-based algorithm are quite similar to the ones provided by the neighboring extremal algorithm.

It should be noted that the numerical algorithms based on the second variation theory—gradient-based algorithm and the neighboring extremal algorithm—provide quite similar results. This fact leads us to suppose that the solutions provided by the both algorithms are really optimal in the sense of a local minimum for the consumption variable J, although the sufficiency conditions are not tested. Besides, we note that the Pontryagin maximum principle is a set of necessary and sufficient conditions for the linearized problem describing the transfers between close circular orbits [26].

6. Conclusion

In this paper, a numerical and analytical study of optimal low-thrust limited-power trajectories for simple transfer (no rendezvous) between close circular coplanar orbits in an inverse-square force field is presented. The numerical study is carried out by means of a neighboring extremal algorithm and the analytical one is based on linear theory obtained through canonical transformation theory, using the concept of generalized canonical systems. The numerical and analytical results have been compared to the ones obtained through a numerical method based on gradient techniques. The great agreement between the results shows that the linear theory provides a good approximation for the
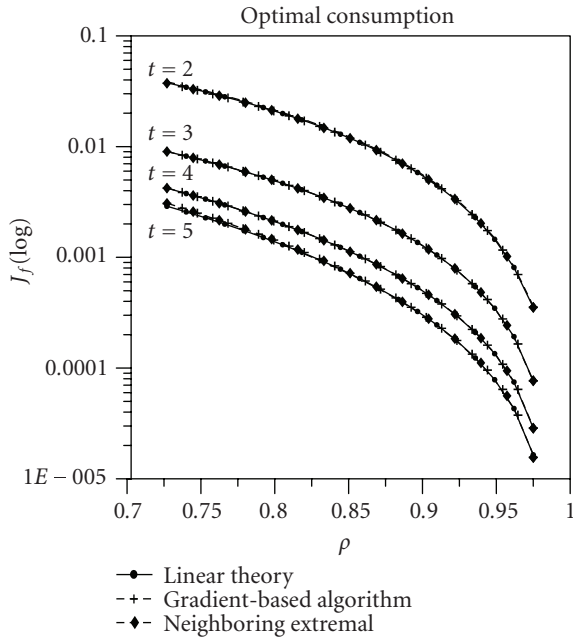
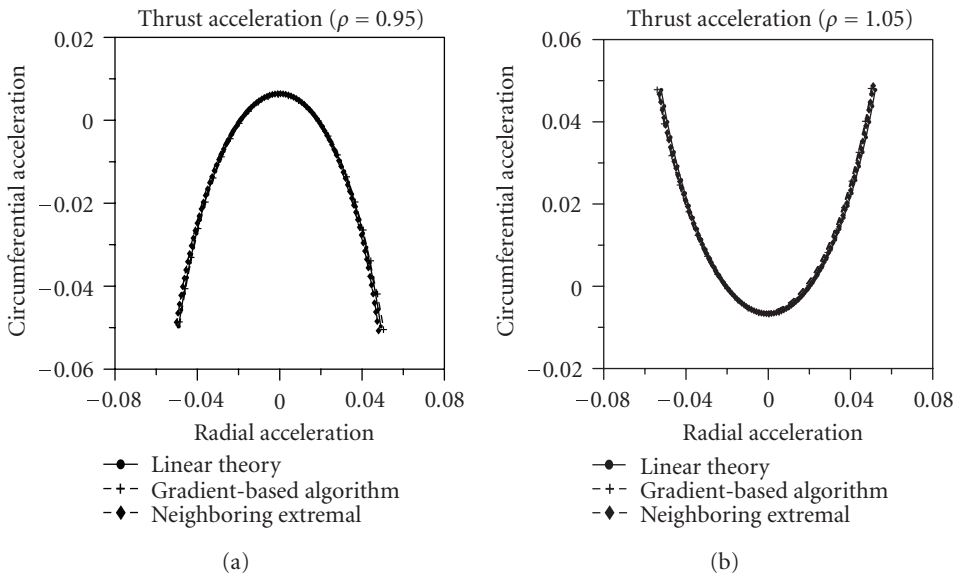Figure 5.2. Consumption variable J for $\rho < 1$.

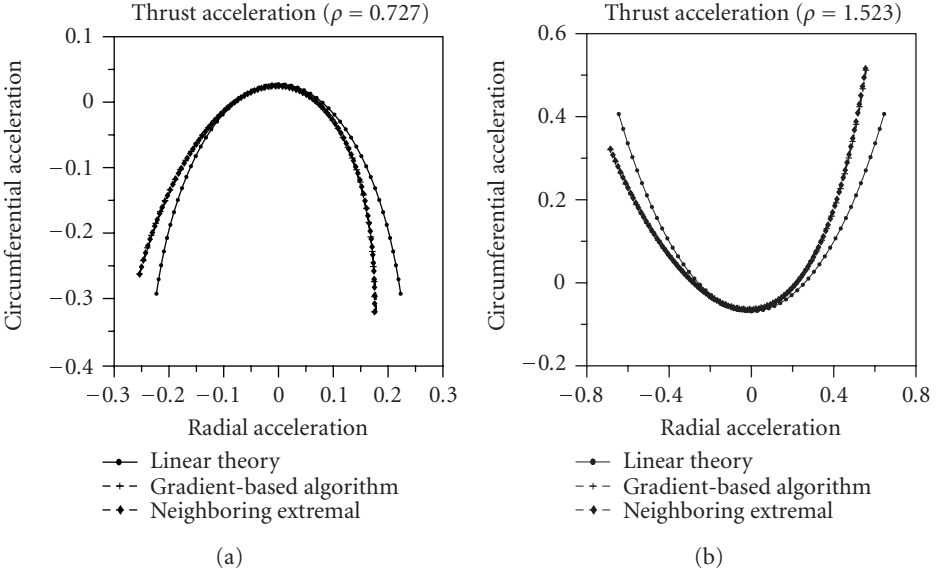Figure 5.3. Thrust acceleration for $t_f - t_0 = 2$ (transfers with small amplitude).

Figure 5.4. Thrust acceleration for $t_f - t_0 = 2$ (transfers with moderate amplitude).

solution of the transfer problem and it can be used in preliminary mission analysis concerning close coplanar circular orbits. On the other hand, the good performance of the algorithms based on the second variation theory shows that they are also good tools in determining optimal low-thrust limited-power trajectories.

Appendix

In this appendix, the modified accessory minimum problem is described. Consider the Bolza problem formulated in Section 2. Introducing the adjoint vector $\lambda(t)$ and the vector of Lagrange multipliers μ, the augmented performance index $\bar{J}$ is formed using (2.3) and (2.4),

$$\bar{J} = g(x(t_f)) + \mu^T \psi(x(t_f)) + \int_{t_0}^{t_f} [-H(x, \lambda, u) + \lambda^T \dot{x}] dt, \tag{A.1}$$

where H is the Hamiltonian function previously introduced in Section 2.

Now, consider the expansion of $\bar{J}$ to second-order and the constraints, defined by (2.2)–(2.4), to first order. Taking into account that all first-order terms vanish about a nominal extremal solution (see (2.5)–(2.10)), one finds that

$$\delta^2 \bar{J} = \frac{1}{2} \delta x^T (t_f) (g_{xx} + \mu^T \psi_{xx}) \delta x(t_f) - \frac{1}{2} \int_{t_0}^{t_f} \{\delta x^T H_{xx} \delta x + 2\delta u^T H_{ux} \delta x + \delta u^T H_{uu} \delta u\} dt, \tag{A.2}$$

(a)

(b)

(c)
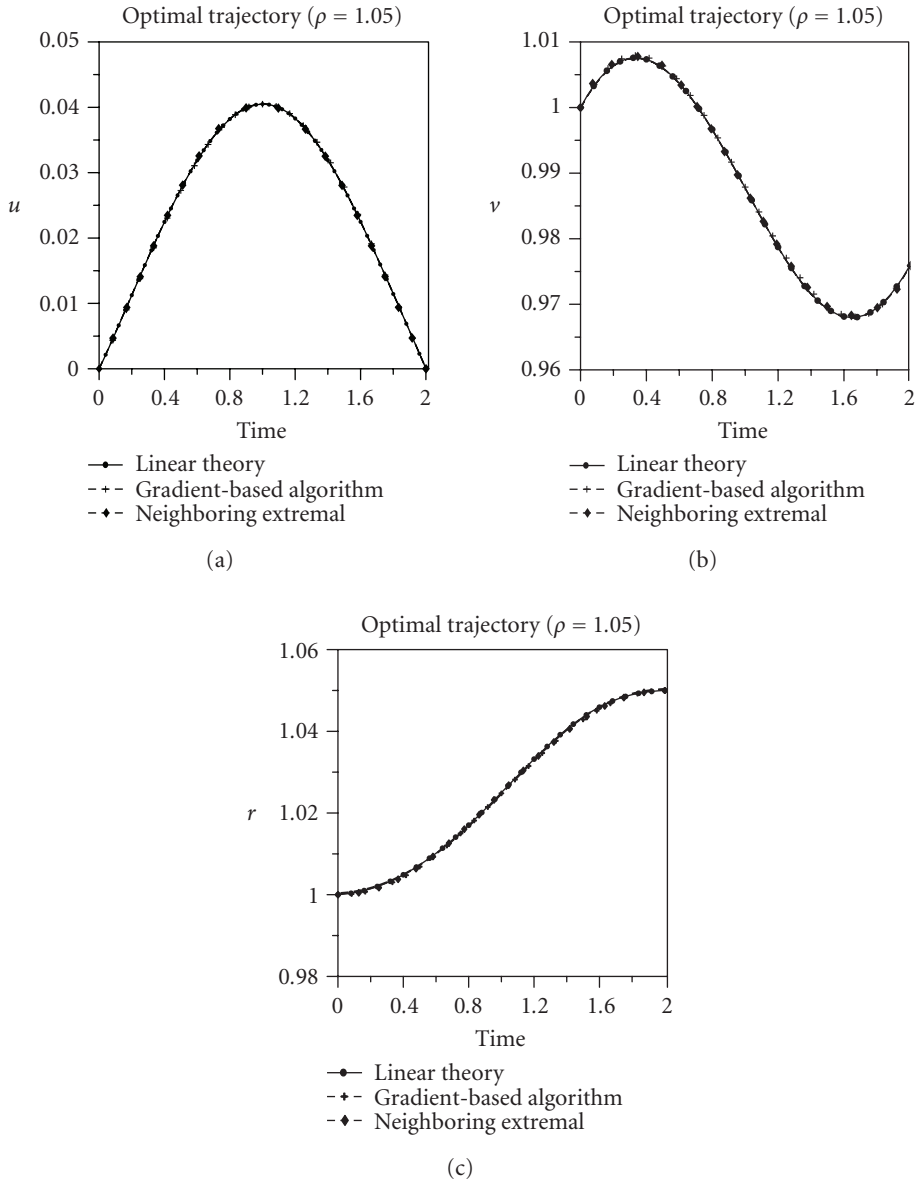
Figure 5.5. Time history of state variables for $t_f - t_0 = 2$ and $\rho = 1.050$.

$$\delta\dot{x} = H_{\lambda x}\delta x + H_{\lambda u}\delta u, \tag{A.3}$$

$$\delta x(t_0) = 0, \tag{A.4}$$

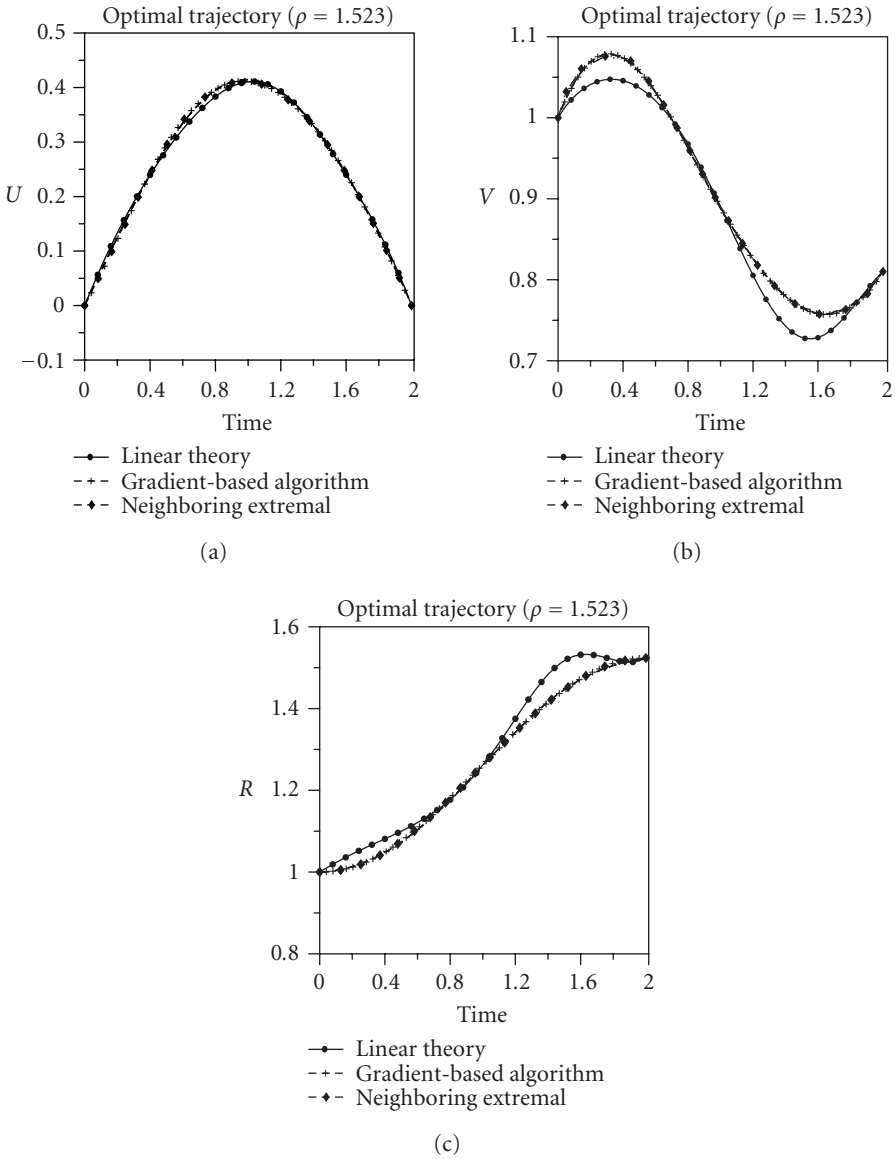$$\psi_x \delta x(t_f) = -k\psi. \tag{A.5}$$

(a)

(b)

(c)

Figure 5.6. Time history of state variables for $t_f - t_0 = 2$ and $\rho = 1.523$.

All quantities, $H_{xx}, H_{\lambda x}, g_{xx}, \psi, \ldots$, in equations above, are evaluated on a nominal extremal solution and k is defined in Section 2.

In order to assure that the expansion above is valid, a constraint is imposed on the control variations:

$$\frac{1}{2} \int_{t_0}^{t_f} \delta u^T W \delta u \, dt = M, \tag{A.6}$$

where $W(t)$ is an arbitrary $m \times m$ positive-definite weighting matrix and $M > 0$ is an arbitrary prescribed value.

Consider the following Bolza problem: determine δu such that $\delta^2 \overline{J}$ is minimized subject to the constraints (A.3) through (A.6). In view of the imposed constraint on the control variations defined by (A.6), this minimization problem is referred to as modified accessory minimum problem. By applying the set of necessary and sufficient conditions to this minimization problem, one finds (2.12) through (2.17), with (2.14) replaced by

$$H_{ux}\delta x + H_{u\lambda}\delta\lambda + (H_{uu} + \alpha W)\delta u = 0, \qquad (A.7)$$

where α is a constant Lagrange multiplier associated to the constraint (A.6). Since W and M are arbitrary, α can be included in the choice of matrix W, that is, a new arbitrary $m \times m$ matrix W_2 can be introduced such that $W_2 = \alpha W$. The evaluation of α is unnecessary, as well as the choice of M. Accordingly, (A.7) can be replaced by

$$H_{ux}\delta x + H_{u\lambda}\delta\lambda + (H_{uu} + W_2)\delta u = 0. \qquad (A.8)$$

Beside the equations mentioned above, the strengthened Legendre condition must be satisfied, that is,

$$H_{uu} + W_2 < 0. \qquad (A.9)$$

Acknowledgment

References

[1] J.-P. Marec, *Optimal Space Trajectories*, Elsevier, New York, NY, USA, 1979.

[2] V. Coverstone-Carroll and S. N. Williams, "Optimal low thrust trajectories using differential inclusion concepts," *Journal of the Astronautical Sciences*, vol. 42, no. 4, pp. 379–393, 1994.

[3] J. A. Kechichian, "Optimal low-thrust rendezvous using equinoctial orbit elements," *Acta Astronautica*, vol. 38, no. 1, pp. 1–14, 1996.

[4] J. A. Kechichian, "Reformulation of Edelbaum's low-thrust transfer problem using optimal control theory," *Journal of Guidance, Control, and Dynamics*, vol. 20, no. 5, pp. 988–994, 1997.

[5] J. A. Kechichian, "Orbit raising with low-thrust tangential acceleration in presence of earth shadow," *Journal of Spacecraft and Rockets*, vol. 35, no. 4, pp. 516–525, 1998.

[6] C. A. Kluever and S. R. Oleson, "A direct approach for computing near-optimal low-thrust transfers," in *AAS/AIAA Astrodynamics Specialist Conference*, Sun Valley, Idaho, USA, August 1997, AAS paper 97-717.

[7] A. A. Sukhanov and A. F. B. A. Prado, "Constant tangential low-thrust trajectories near an oblate planet," *Journal of Guidance, Control, and Dynamics*, vol. 24, no. 4, pp. 723–731, 2001.

[8] V. Coverstone-Carroll, J. W. Hartmann, and W. J. Mason, "Optimal multi-objective low-thrust spacecraft trajectories," *Computer Methods in Applied Mechanics and Engineering*, vol. 186, no. 2–4, pp. 387–402, 2000.

[9] M. Vasile, F. B. Zazzera, R. Jehn, and G. Janin, "Optimal interplanetary trajectories using a combination of low-thrust and gravity assist manoeuvres," in *Proceedings of the 51st International Astronautical Congress (IAF '00)*, Rio de Janeiro, Brazil, October 2000, IAF-00-A.5.07.

[10] G. D. Racca, "New challenges to trajectory design by the use of electric propulsion and other new means of wandering in the solar system," *Celestial Mechanics & Dynamical Astronomy*, vol. 85, no. 1, pp. 1–24, 2003.

[11] T. N. Edelbaum, "Optimum power-limited orbit transfer in strong gravity fields," *AIAA Journal*, vol. 3, no. 5, pp. 921–925, 1965.

[12] J.-P. Marec and N. X. Vinh, "Optimal low-thrust, limited power transfers between arbitrary elliptical orbits," *Acta Astronautica*, vol. 4, no. 5-6, pp. 511–540, 1977.

[13] C. M. Hassig, K. D. Mease, and N. X. Vinh, "Minimum-fuel power-limited transfer between coplanar elliptical orbits," *Acta Astronautica*, vol. 29, no. 1, pp. 1–15, 1993.

[14] S. Geffroy and R. Epenoy, "Optimal low-thrust transfers with constraints—generalization of averaging techniques," *Acta Astronautica*, vol. 41, no. 3, pp. 133–149, 1997.

[15] B. N. Kiforenko, "Optimal low-thrust orbital transfers in a central gravity field," *International Applied Mechanics*, vol. 41, no. 11, pp. 1211–1238, 2005.

[16] J. V. Breakwell, J. L. Speyer, and A. E. Bryson Jr., "Optimization and control of nonlinear systems using the second variation," *SIAM Journal on Control and Optimization*, vol. 1, no. 2, pp. 193–223, 1963.

[17] A. G. Longmuir and E. V. Bohn, "Second-variation methods in dynamic optimization," *Journal of Optimization Theory and Applications*, vol. 3, no. 3, pp. 164–173, 1969.

[18] J.-P. Marec, *Transferts Optimaux Entre Orbites Elliptiques Proches*, ONERA, Châtillon, France, 1967.

[19] S. da Silva Fernandes and W. A. Golfetto, "Numerical computation of optimal low-thrust limited-power trajectories—transfers between coplanar circular orbits," *Journal of the Brazilian Society of Mechanical Sciences and Engineering*, vol. 27, no. 2, pp. 178–185, 2005.

[20] S. da Silva Fernandes and W. A. Golfetto, "Computation of optimal low-thrust limited-power trajectories through an algorithm based on gradient techniques," in *Proceedings of the 3rd Brazilian Conference on Dynamics, Control and Their Applications*, pp. 789–796, São Paulo, Brazil, 2004, CD-ROM.

[21] A. E. Bryson Jr. and Y. C. Ho, *Applied Optimal Control*, John Wiley & Sons, New York, NY, USA, 1975.

[22] L. S. Pontryagin, V. G. Boltyanskii, R. V. Gamkrelidze, and E. F. Mishchenko, *The Mathematical Theory of Optimal Processes*, John Wiley & Sons, New York, NY, USA, 1962.

[23] T. Bullock and G. Franklin, "A second-order feedback method for optimal control computations," *IEEE Transactions on Automatic Control*, vol. 12, no. 6, pp. 666–673, 1967.

[24] S. da Silva Fernandes, "A note on the solution of the coast-arc problem," *Acta Astronautica*, vol. 45, no. 1, pp. 53–57, 1999.

[25] S. da Silva Fernandes, "Generalized canonical systems applications to optimal trajectory analysis," *Journal of Guidance, Control, and Dynamics*, vol. 22, no. 6, pp. 918–921, 1999.

[26] F. W. Gobetz, "A linear theory of optimum low-thrust rendez-vous trajectories," *The Journal of the Astronautical Sciences*, vol. 12, no. 3, pp. 69–76, 1965.

Sandro da Silva Fernandes: Departamento de Matemática, Instituto Tecnológico de Aeronáutica, 12228-900 São José dos Campos, SP, Brazil
Email address: sandro@ita.br

Wander Almodovar Golfetto: Instituto de Aeronáutica e Espaço, Comando Geral de Tecnologia Aeroespacial, 12228-904 São José dos Campos, SP, Brazil
Email address: wander@iae.cta.br